Available online at www.sciencedirect.com
ScienceDirect
Phytochemistry 69 (2008) 1339–1347
PHYTOCHEMISTRY
www.elsevier.com/locate/phytochem

Phytotoxic activity and conformational analysis of thymol analogs from *Hofmeisteria schaffneri* ☆

Araceli Pérez-Vásquez [a], Edelmira Linares [b], Robert Bye [b], Carlos M. Cerda-García-Rojas [c,*], Rachel Mata [a,*]

[a] *Facultad de Química, Universidad Nacional Autónoma de México, México DF 04510, Mexico*
[b] *Instituto de Biología, Universidad Nacional Autónoma de México, México DF 04510, Mexico*
[c] *Departamento de Química, Centro de Investigación y de Estudios Avanzados del Instituto Politécnico Nacional, México DF 07000, Mexico*

Received 15 August 2007; received in revised form 21 December 2007
Available online 6 March 2008

Abstract

Bioassay-guided fractionation of two phytotoxic extracts (a CH_2Cl_2–MeOH (1:1) and an aqueous) prepared from the aerial parts of *Hofmeisteria schaffneri* led to isolation of thymol analogs **3**–**5**, along with seven known compounds, **1**, **2** and **6**–**10**. Compounds **3**–**5** were identified by spectroscopic methods as 1,4-bis(2′-hydroxy-4′-methylphenyl)butane-1,4-dione (**3**), 2-isopropyl-5-methylphenyl (2*Z*)-2-methylbut-2-enoate (**4**) and 2-hydroxy-2-(2-hydroxy-4-methylphenyl)propane-1,3-diyl (2*Z*,2′*Z*)bis(2-methylbut-2-enoate) (**5**) and designated trivial names of hofmeisterins II–IV, respectively. Their conformational behavior was also studied by molecular modeling using density functional theory calculations at the B3LYP/DGDZVP level. Compounds **1**–**4** and **6**–**10** significantly inhibited radicle growth of seedlings of *Amaranthus hypochondriacus* and *Echinochloa crus-galli* in the Petri dish bioassay with IC_{50}'s $\leqslant 10^{-4}$ M. Furthermore, the northymol analog **3** provoked significant bleaching of seedlings of *A. hypochondriacus*. However, none of the isolates affected either seedling growth or germination of *Medicago sativa*.

Keywords: *Hofmeisteria schaffneri*; Asteraceae; *Amaranthus hypochondriacus*; *Amaranthaceae*; *Echinochloa crus-galli*; Gramineae; *Medicago sativa*; Leguminosae; Phytotoxicity; Thymol derivatives; Hofmeisterins I-IV; Conformational analysis; DFT calculations

1. Introduction

Hofmeisteria schaffneri (A. Gray) R.M. King and H. Robinson (Asteraceae) is a medicinal herb which grows naturally in the oak and pine-oak forested mountains of the central Mexican states of Jalisco and San Luis Potosi. It is also cultivated in home gardens in the State of Mexico, Mexico City, and Michoacan. The decoction of the fresh, leafy stems and flowers is used medicinally for treating skin wounds, fevers, and gastrointestinal ailments (Pérez-Vásquez et al., 2005).

As part of our research program to discover new potential herbicidal agents from Mexican plants (Valencia-Islas et al., 2002a, 2002b; Hernández-Romero et al., 2005, inter alia), *H. schaffneri* was selected for bioassay-guided fractionation on the basis of its significant phytotoxic effect against *Amaranthus hypochondriacus* L. (Amaranthaceae) and *Echinochloa crus-galli* (L.) P. Beauv. (Poaceae) seedlings. Bioassay-guided fractionation of the active extract yielded two potent calmodulin-inhibitors with phytotoxic properties, namely hofmeisterin (**1**) and the dimer **2** (Pérez-Vásquez et al., 2005). An efficient synthesis of **1** was also developed (Pérez-Vásquez et al., 2005).

Continuing with the search of *H. schaffneri* as a source of phytotoxic agents, this work was undertaken to isolate the active principles present in an aqueous leaching and a CH_2–Cl_2–MeOH 1:1 extract prepared from a new

☆ Taken in part from the Ph.D thesis of A. Pérez-Vásquez.
* Corresponding authors. Tel.: +525 55 622 5289; fax: +525 55 622 5329.
E-mail addresses: ccerda@cinvestav.mx (C.M. Cerda-García-Rojas), rachel@servidor.unam.mx (R. Mata).

0031-9422/$ - see front matter © 2008 Elsevier Ltd. All rights reserved.
doi:10.1016/j.phytochem.2008.01.011

collection of the plant. Herein, we describe the isolation, structure elucidation, and phytotoxic activity of thymol analogs **3**–**9** and thymol itself (**10**). In addition, the conformational analysis of **1**–**5**, using density functional theory (DFT), is described.

2. Results and Discussions

Bioassay guided fractionation of a phytotoxic CH_2Cl_2–MeOH (1:1) extract (see Table 1) from a new collection of *H. schaffneri* resulted in isolation of two new naturally occurring thymol analogs, namely 1,4-bis(2′-hydroxy-4′-methylphenyl)butane-1,4-dione (**3**) and 2-isopropyl-5-methylphenyl (2*Z*)-2-methylbut-2-enoate (**4**), along with the known compounds **1**, **2** and **9** (Fig. 1). Compounds **3** and **4** were designated the trivial names of hofmeisterins II and III, respectively. On the other hand, phytotoxic aqueous leachates (Table 1), prepared from the fresh aerial parts of the plant, yielded monoterpenoids **5**–**8** and **10** (Fig. 1). Compound **5**, designated with the trivial name of hofmeisterin IV, was newly isolated and characterized as 2-hydroxy-2-(2-hydroxy-4-methylphenyl)propane-1,3-diyl (2*Z*,2'*Z*)bis(2-methylbut-2-enoate) (**5**).

Compounds **7** and **9** were previously obtained from *Eupatorium fortunei* (Tori et al., 2001) while **6** and **8** from *E. stoechadosmum* (Nguyen et al., 1993) and *Doronicum hungaricum* (Bohlmann et al., 1980); the three species belong also to the Asteraceae family. The spectroscopic properties of **6–10** were in accordance with those earlier reported. The new thymol analogs **3**–**5** were characterized by the analysis of their spectroscopic and spectrometric data as well as by the X-ray diffraction of **3**.

X-ray analysis of **3** (Fig. 2) established its structure, including the anti-arrangement of the 1,4-butanedione moiety. Interestingly, Passreiter et al. (2002) obtained compound **3** as the major component of a mixture that resulted from oxidation of **2** with $K_2Cr_2O_7$. However, this is the first report of its isolation from a natural source. For synthetic **3**, however, UV and IR data were not provided and the NMR spectroscopic assignments were not described. Therefore, this information is included in the experimental.

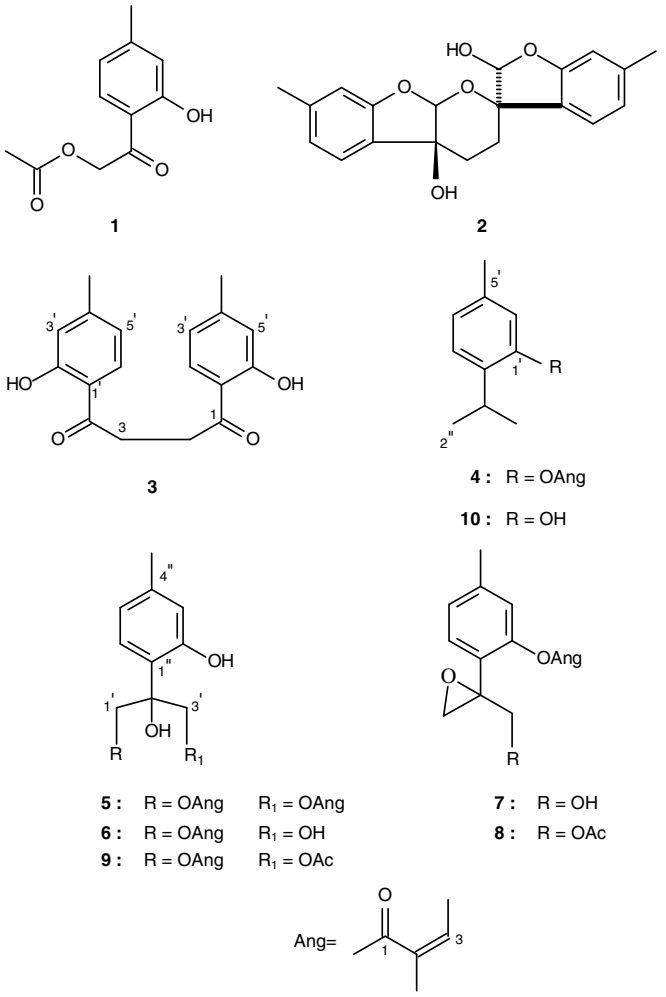

Fig. 1. Structure of thymol derivatives (**1**–**10**) from *Hofmeisteria schaffneri*.

Table 1
Phytogrowth-inhibitory activity (IC_{50}, M) of the extracts and compounds (**1**–**4** and **6**–**10**) from *H. schaffneri*

Extracts/compounds	*A. hypochondriacus* seedling growth IC_{50} (M)	*E. crus-galli*	*M. sativa*
Aqueous	126.7[b]	179.2[b]	>1000[b]
CH_2Cl_2–MeOH (1:1)	59.0[b]	107.7[b]	>1000[b]
1	3.5×10^{-6}	5.67×10^{-3}	$>1 \times 10^{-3}$
2	9.3×10^{-7}	4.2×10^{-4}	$>1 \times 10^{-3}$
3	4.16×10^{-4}	8.6×10^{-5}	$>1 \times 10^{-3}$
4	1.38×10^{-4}	1.17×10^{-6}	$>1 \times 10^{-3}$
5	ND[c]	ND[c]	ND[c]
6	9.1×10^{-4}	5.2×10^{-4}	$>1 \times 10^{-3}$
7	12.7×10^{-4}	ND[c]	ND[c]
8	6.4×10^{-4}	1.16×10^{-4}	4.25×10^{-3}
9	7.4×10^{-4}	21.0×10^{-4}	8.21×10^{-3}
10	1.4×10^{-5}	3.6×10^{-5}	$>1 \times 10^{-3}$
Tricolorin A[a]	3.61×10^{-5}	1.1×10^{-5}	5.1×10^{-4}

[a] Positive standard control.
[b] Expressed in $\mu g\ mL^{-1}$.
[c] Not determined due to the scarcity of the sample.

Compound **4** (Table 2) was identified as 2-isopropyl-5-methylphenyl (2*Z*)-2-methylbut-2-enoate, an ester of angelic acid. The presence of an angeloyl residue in **4** was established by comparison of the ^1H and ^{13}C NMR chemical shifts of the acid residue with those previously described for other angeloyl derivatives (Joseph-Nathan et al., 1984). Thus, in compound **4**, the ^{13}C NMR chemical shifts for the methyl groups were observed at δ_C 15.9 and 20.7, whereas the signal for H-3 appeared at δ 6.23 in the ^1H NMR spectrum. A NOE differential experiment (Joseph-Nathan et al., 1984; Tori et al., 2001) corroborated the existence in the molecule of an angeloyl group since irradiation of the vinylic hydrogen signal at δ_H 6.23 resulted in a enhancement of the resonance for the methyl groups at δ_H 2.07 and 2.09.

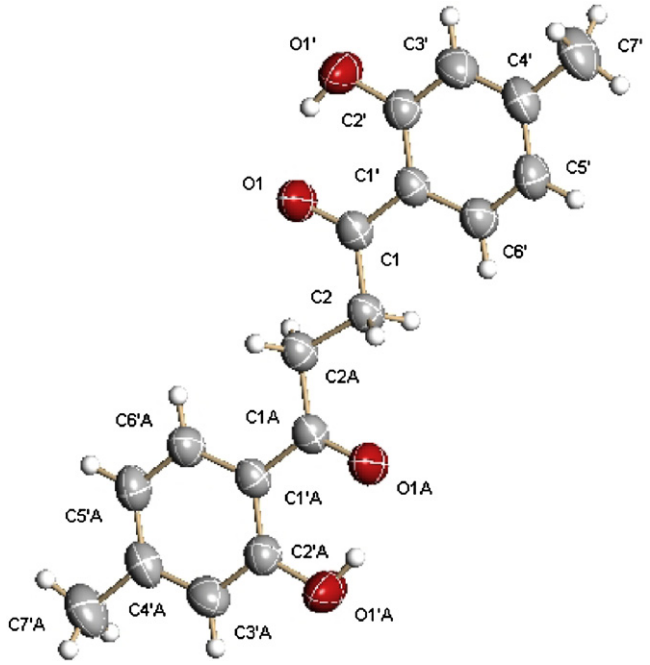

Fig. 2. X-ray structure of hofmeisterin II (**3**).

Compound **5** was isolated as colorless oil. Its NMR spectra showed similarities (Table 3), albeit partial, with compound **6** (Tori et al., 2001). The main difference between the NMR spectra of compounds **6** and **5** was the absence of the signals due to a hydroxymethylene group in the latter, which were replaced by an additional angeloyloxy methylene moiety (see Table 3). Consequently, compound **5** had two angeloyloxy residues

As part of their structural characterization, conformational analyses of the new compounds **3**–**5** using molecular modeling techniques were carried out. The analysis was extended to **1** and **2** considering that this information would be useful for future studies regarding the mode of action of these compounds at the molecular level.

First, a preliminary searching protocol using the Monte Carlo method (Chang et al., 1989) was carried out; then,

Table 2
^{1}H (300 MHz) and ^{13}C (75 MHz) NMR spectroscopic data of **4** ($CDCl_3$)

C	δ_H *J* (Hz)	δ_C	HMBC (H → C)
1	–	166.0	–
2	–	127.3	–
3	6.23 *m*	140.3	–
4	2.07 *sa*	20.7	3
2–CH_3	2.09 *sa*	15.9	1, 3
1′	–	147.0	–
2′	–	136.5	–
3′	7.21 *d* (7.8)	126.3	1′, 2′, 4′
4′	7.01 *br d* (7.8)	126.9	5′, 5′–CH_3
5′	–	137.0	–
6′	6.85 *br s*	122.9	5′–CH_3,
5′–CH_3	2.32 *s*	20.8	4′, 5′, 6′
1″	2.98 *h* (6.9)	27.2	1′, 2′, 3′, 2″, 3″
2″	1.20 *s*	22.9	2′
3″	1.18 *s*	22.9	2′

Table 3
^{1}H (500 MHz) and ^{13}C (125 MHz) NMR spectroscopic data of **5** ($CDCl_3$)

C	δ_H *J* (Hz)	δ_C	HMBC (H → C)
1	–	168.1	–
2	–	127.0	–
3	6.12 *qq* (7.1, 1.5)	140.0	2, 4
4	1.93 *dq* (7.1, 1.5)	15.8	3
2–CH_3	1.85 *q* (1.5)	20.5	3
1′, 3′	4.55 *s*	67.6	6′
2′	–	78.9	–
1″	–	118.9	–
2″	–	156.8	–
3″	6.7 *m*	118.7	1′, 3′, 5″ 2″–OH
4″	–	140.1	–
5″	6.65 *ddd* (8, 1.5, 0.5)	120.4	–
6″	6.94 *d* (10)	126.5	5″
4″–CH_3	2.26 *br s*	20.9	5″, 6″
2″–OH	8.86 *s*	–	

conformational analyses of compounds **1**–**5** were performed using density functional theory (DFT) calculations at B3LYP/DGDZVP level theory. The latter takes into account valence polarization and diffuse functions. It was selected, because of the presence in these molecules of delocalized electron systems containing oxygen atoms.

The Monte Carlo analysis indicated a total of 17, 11, 42, 4 and 77 minimum energy conformations for compounds **1**–**5**, respectively. The molecular mechanics structures were analyzed to eliminate those which appeared to be duplicated, and they were sorted according to their energy. For compounds **4** and **5**, a geometric restriction for the C=C–C=O torsion angle of the angelate esters was set at 0°, in order to emulate the π-electron conjugation effect (Jiménez-Estrada et al., 1989; Román et al., 1981; Cerda-García-Rojas et al., 2006). This restriction was applied at the beginning of the calculation process. Next, a selection of minimum energy structures, within the range from 0 to 3 kcal/mol, was submitted to geometry optimization by DFT calculation without any geometrical restriction. After these calculations, sets of 7, 8, 6, 4 and 12 conformations for structures **1**–**5**, respectively, were considered for the Boltzmann population analysis. Enthalpy and particularly entropy are very relevant factors to be considered in the conformational study of these structures. Table 4 summarizes the thermochemical parameters ΔE_0, ΔE_{298}, ΔH_{298}, and ΔG_{298} employed in the estimation of the population for each conformer, which was calculated according to the $\Delta G = \Delta H - T\Delta S$ and $\Delta G = -RT\ln K$ equations, considering the B3LYP/DGDZVP calculated frequencies at 298 K and 1 atm. The DFT global and the second minimum structures for each compound are depicted in Fig. 3 showing the corresponding population, while in Fig. 4 the superimposed minimum energy structure sets evidence the high mobility of these natural substances.

It is worth mentioning that the solid state structure of **3** was very close to the second minimum structure **3b** (Fig. 3), while the global minimum **3a** adopted a syn-arrangement which is stabilized by the entropic term (Table 4). In contrast, the global minimum structure **2a**, with the tetrahy-

Table 4
DFT thermochemical parameters and population for the more relevant minimum energy structures[a] of compounds **1–5**

Conformer	ΔE_0[b,c]	ΔE_{298}[c]	ΔH_{298}[c]	ΔG_{298}[c]	p_{DFT}[d]
1[a]	0.0000	0.0000	0.0000	0.0000	32.13
1b	0.0006	−0.0006	0.0000	0.0063	31.79
1c	1.1408	1.3071	1.3077	0.3006	19.34
1d	1.4019	1.5117	1.5117	0.7869	8.51
1e	1.4050	1.5123	1.5129	0.8070	8.23
2[a]	0.0000	0.0000	0.0000	0.0000	58.16
2b	1.0479	1.0285	1.0285	0.6714	18.73
2c	−0.1060	−0.6783	−0.6783	1.1923	7.77
2d	1.2406	1.2337	1.2337	1.3197	6.27
2e	1.9127	1.9108	1.9108	1.5914	3.96
2f	1.4878	1.5136	1.5136	1.6284	3.72
2g	2.2829	2.3036	2.3036	2.2151	1.38
3[a]	0.0000	0.0000	0.0000	0.0000	35.52
3b	−0.4506	−0.3539	−0.3533	0.0973	30.14
3c	−0.0220	−0.0182	−0.0182	0.4010	18.05
3d	0.1694	0.1205	0.1211	0.6357	12.15
3e	1.3040	1.3272	1.3272	1.2726	4.15
4[a]	0.0000	0.0000	0.0000	0.0000	67.69
4b	0.0584	0.0213	0.0213	0.5177	28.25
4c	1.2098	1.1427	1.1427	2.0312	2.20
4d	1.2155	1.1383	1.1389	2.1285	1.86
5[a]	0.0000	0.0000	0.0000	0.0000	59.41
5b	−0.1431	−0.1826	−0.1826	0.4217	29.16
5c	0.1211	−0.0038	−0.0031	1.1396	8.68
5d	0.6589	0.5020	0.5020	2.0902	1.74
5e	1.1195	1.0084	1.0090	2.4134	1.01

[a] Covering >99% of the conformational population.
[b] Sum of electronic and zero-point DFT B3LYP/DGDZVP energies in kcal/mol relative to the global minimum calculated at 298 K and 1 atm.
[c] For **1a** the absolute values are $E_0 = -727.198102$, $E_{298} = -727.183375$, $H_{298} = -727.182431$, $G_{298} = -727.241839$ au. For **2a** the absolute values are $E_0 = -1150.048173$, $E_{298} = -1150.026567$, $H_{298} = -1150.025623$, $G_{298} = -1150.099582$ au. For **3a** the absolute values are $E_0 = -997.478755$, $E_{298} = -997.458211$, $H_{298} = -997.457267$, $G_{298} = -997.531726$ au. For **4a** the absolute values are $E_0 = -733.857928$, $E_{298} = -733.838880$, $H_{298} = -733.837936$, $G_{298} = -733.908021$ au. For **5a** the absolute values are $E_0 = -1228.850431$, $E_{298} = -1228.822094$, $H_{298} = -1228.821150$, $G_{298} = -228.915035$ au.
[d] DFT population in % calculated from ΔG_{298} values.

dropyran ring adopting a boat conformation, was very similar to that found in the solid state by Passreiter and coworkers (2002). On the other hand, in the second minimum structure **2b**, this ring adopts a chair conformation. It is relevant to mention that in the molecular mechanics search, which only takes in to account steric effects, structure **2b** was by far more stable ($\Delta E_{MMFF} = 1.807$ kcal/mol) than **2a**. Therefore, electronic effects should play an important role in the stability of **2a**.

Finally, to validate the conformational equilibrium present in solution for structures **1–5**, the calculated and experimental infrared frequencies were compared as depicted in Fig. 5. The calculated frequencies were obtained by a weighted-averaged combination of the individual frequencies of each conformer according to their molar fraction (Table 4). The very good agreement between the two sets of parameters indicated that the B3LYP/DGDZVP model is accurate. Thus, the molecular modeling study of **1–5** shows important geometrical and dynamic aspects of these relevant natural substances.

The phytotoxic activity of compounds **1–4** and **6–10** was assessed with the Petri dish assay using seedlings of *A. hypochondriacus, E. crus-galli* and *M. sativa.* Tricolorin A, a potent phytotoxic agent from *Ipomoea tricolor* (Convolvulaceae) was selected as a positive control (Pereda-Miranda et al., 1993). According to the results in Table 1, this compound proved to be highly phytotoxic to all the species tested. In general, the thymol analogs evaluated showed a similar spectrum of plant sensitivity, but with differing intensities. Thus, compounds **1–4** and **6–10** significantly inhibited radicle growth of seedlings of *A. hypochondriacus*, with compound **2** the most active. Interestingly, only compound **3**, as noted earlier for several natural β-triketones and sulcotrione (Meazza et al., 2002), provoked significant bleaching of the seedlings of *A. hypochondriacus* at all concentrations tested. *E. crus-galli*, on the other hand, was particularly sensitive to compounds **4**, **3** and **10**. In contrast, even at the highest concentrations used, the tested terpenoids **1–4** and **6–10** were inactive to *M. sativa.*

With regard to **3**, further work is in progress to determine the molecular target of its bleaching effect. The phytotoxic properties of **10** have been previously described using seedlings of several economic plants (Angelini et al., 2003; Vokou et al., 2003; Veronneau et al., 1997). The degree of phytotoxicity provoked by **10** in the present investigation is in agreement with that previously described.

3. Concluding remarks

H. schaffneri biosynthesizes phytotoxic thymol derivatives being northymol **1–4** the most promising as potential herbicide agents against grass weeds.

Thymol and nor-thymol derivatives **1–9** can be biogenetically interrelated starting from a suitable intermediate such as 2-[2-(hydroxymethyl)oxiran-2-yl]-5-methylphenol. This compound could undergo an oxidative cleavage to afford the northymol derivative 2-hydroxy-1-(2-hydroxy-4-methylphenyl)ethanone, which upon appropriate "tailoring" reactions would yield **1**. 2-Hydroxy-1-(2-hydroxy-4-methylphenyl)ethanone could dimerize through an oxidative coupling reaction to generate **3**. Alternatively, compound **3** could arise from dimer **2** by an oxidative degradation reaction, probably an *in vivo* version of the reaction carried out by (Passreiter et al., 2002). Finally, nucleophilic epoxide opening of 2-[2-(hydroxymethyl)oxiran-2-yl]-5-methylphenol would favor the biosynthesis of compounds **5**, **6** and **9**.

Dimer **3** is the second northymol derivative described in *H. schaffneri* and the fourth described in nature. All of them have been isolated from species of the Asteraceae family (Nguyen et al., 1993; Tori et al., 2001; Pérez-Vásquez et al., 2005).

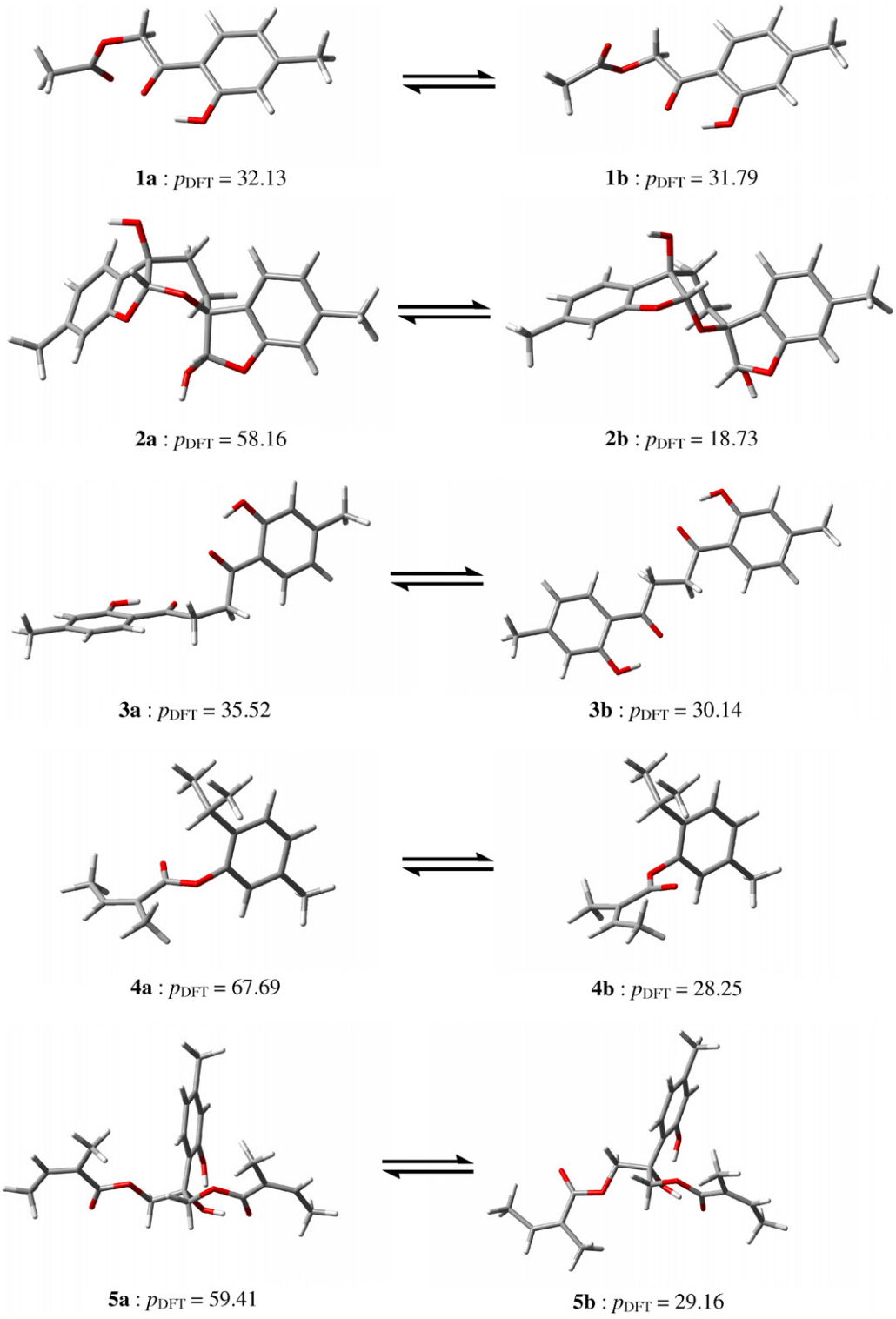

Fig. 3. The global and the second minimum energy structures of **1**–**5** optimized at DFT B3LYP/DGDZVP level of theory. The relative populations are in %.

4. Experimental

4.1. General

Melting points were determined using a Fisher–Johns apparatus and are uncorrected. Optical rotations were recorded on a JASCO DIP 360 digital polarimeter in $CHCl_3$. IR spectra were obtained using KBr disks or films on a Perkin–Elmer 599B spectrophotometer. UV spectra were recorded on a Shimadzu 160 UV spectrometer in CH_2Cl_2 solution. NMR spectra including NOE differential, COSY, HMBC and HMQC experiments were recorded in

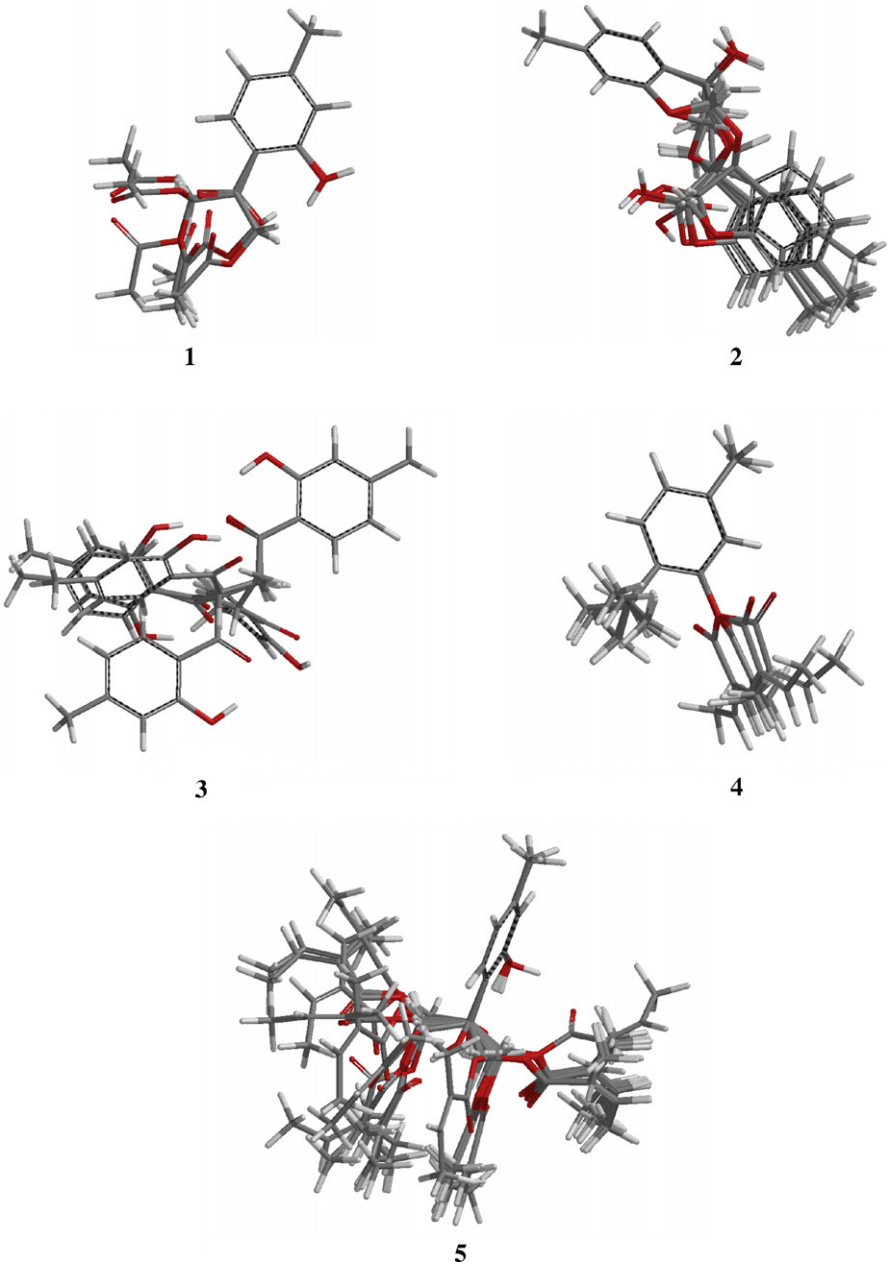

Fig. 4. Superposition of conformers for compounds **1**–**5** obtained by the Monte Carlo method. Minimum energy structures were selected within a range of 0–3 kcal/mol.

$CDCl_3$ either on a Varian Unity Plus 500 spectrometer or on a Bruker DMX500 spectrometer operating at 500 or 300 MHz (^1H) or 125 or 75 MHz (^{13}C) NMR, using tetramethylsilane (TMS) as an internal standard. HREI and FABMS were obtained on a JEOL JMS-AX505HA mass spectrometer. For FAB spectra NBA was used as the matrix.

4.2. Plant material

H. schaffneri was collected in February 2006 from cultivated plants near Ozumba, State of Mexico. A voucher specimen (Bye and Linares 34431) has been deposited in the National Herbarium (MEXU), Instituto de Biología, Universidad Nacional Autónoma de México.

4.3. Extraction and isolation

4.3.1. Extraction and isolation from a CH_2Cl_2–MeOH (1:1) extract of *H. schaffneri*

The CH_2Cl_2–MeOH (1:1) extract (340 g) was obtained by macerating air-dried aerial parts of *H. schaffneri* (1.5 kg) at room temperature during 15 days. The extract was subjected to silica gel CC eluting with hexane–CH_2Cl_2 (10:0 → 0:10) followed by CH_2Cl_2–MeOH (10:0 → 0:10) gradient to yield nine major fractions (F1–F9). According

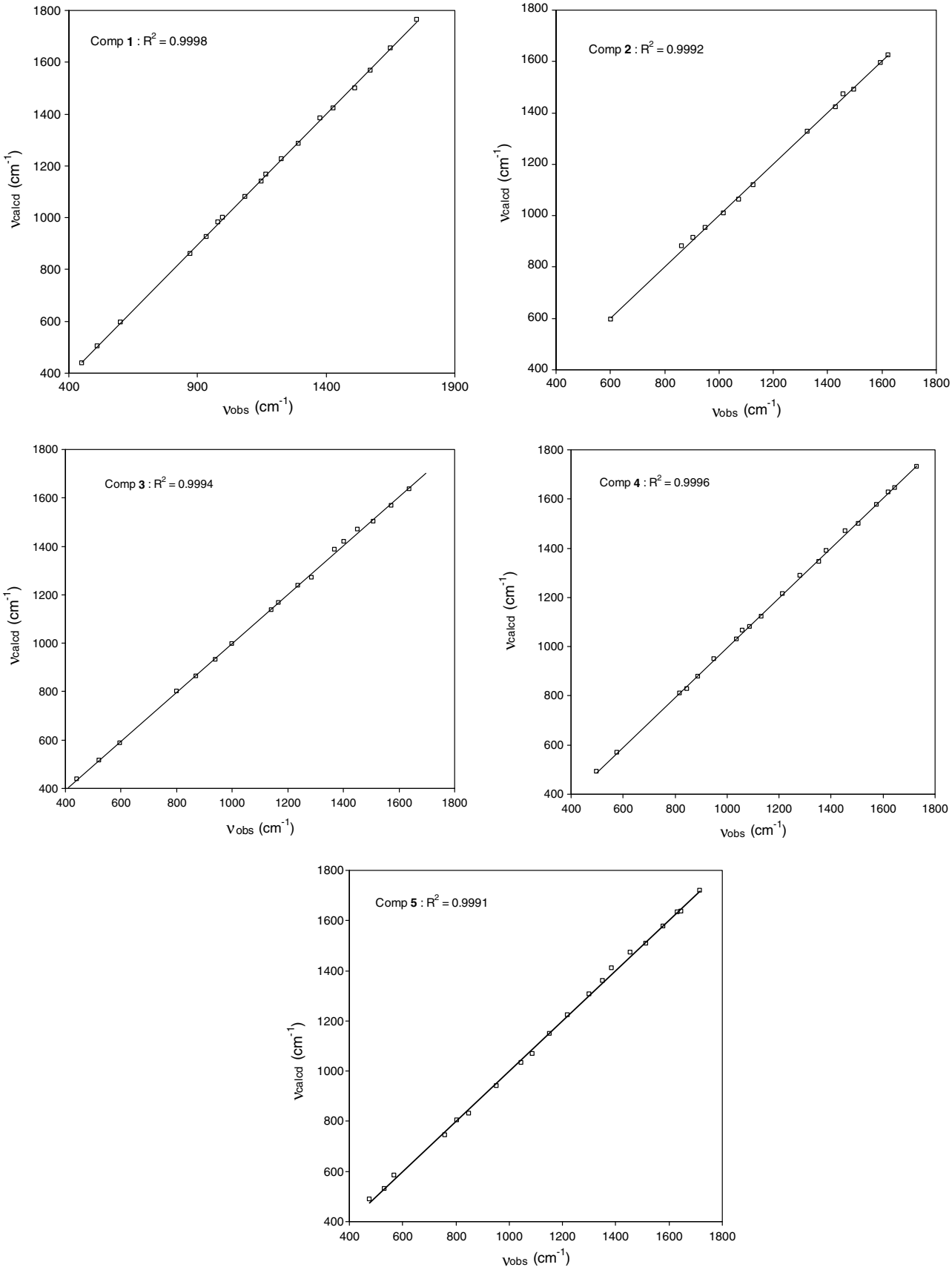

Fig. 5. Comparison between calculated and experimental infrared frequencies for compounds **1**–**5**.

to the bioautographic assay, fractions F3 and F4 were active. Primary fraction F3 (4 g, eluted with hexane–CH_2Cl_2, 2:3) was applied to a silica gel (90 g) column, eluting with hexane EtOAc 96:4 to afford 600 mg of **4** and 18 mg of **10**. Primary fraction F4 (13 g, eluted with CH_2Cl_2) was further subjected to open CC on Si gel (200 g) using hexane–EtOAc (10:0 → 0:10) to yield twenty-five secondary fractions (F4-1–F4-25). Secondary fraction F4-17 (0.88 g, eluted with hexane EtOAc 85:15) was further applied to a silica gel (80 g) column, eluted with a gradient of hexane–EtOAc (10:0 → 0:10) to yield eight tertiary fractions (F4-17-1–F4-17-8). Fraction F4-17-1 (90 mg) was purified by preparative TLC (CH_2Cl_2–MeOH 9.6:0.4) to yield **9** (41 mg). Secondary fraction F4-14 (1.65 g, eluted hexane EtOAc 9:1) was further purified by silica gel (126 g) CC, eluting with a gradient of hexane–EtOAc (10:0 → 0:10) to yield twenty-two fractions (F4-14-1–F4-14-22). From fraction F4-14-2, compound **3** (34 mg) spontaneously crystallized. From fraction F4-18, compound **1** (10 mg) spontaneously crystallized which was identical to an authentic sample (Pérez-Vásquez et al., 2005). Finally from fraction F-4-18, compound **2** (160 mg) crystallized; it was identical to an authentic sample (Pérez-Vásquez et al., 2005).

4.3.2. Extraction and isolation from an aqueous extract of H. schaffneri

The aqueous extract was prepared by treating air-dried aerial parts (108 g) of *H. schaffneri* with hot H_2O (3 l) for 30 min. The resulting aqueous extract was exhaustively partitioned with CH_2Cl_2 (3 l × 3). The resulting organic phase was dried over anhydrous Na_2SO_4 and concentrated *in vacuo* to yield a brown residue (1.2 g). The residue was subjected to Sephadex LH-20 (MeOH) CC to yield seven fractions (1-A–1-G). Fraction 1-D (470 mg) was further purified on Sephadex LH-20 (MeOH) CC to yield 21 fractions (1-D-1–1-D-21). Fraction 1-D-10 (130 mg) was purified by preparative TLC (CH_2Cl_2:MeOH 9.6:0.4) to yield compounds **8** (15 mg), **10** (8 mg), **7** (11 mg) and **5** (5 mg) as glassy solids. Fraction 1-D-16 was also resolved by preparative TLC (CH_2Cl_2:MeOH 9.6:0.4) to yield **6** (15 mg) as glassy solid.

4.4. Characterization

4.4.1. Hofmeisterin II (3)

Colorless crystalline needles; m.p. 193 °C; UV (CH_2Cl_2) λ_{max} nm (log ε): 264 (4.58), 326 (4.08); IR (KBr) ν_{max} cm^{-1}: 3417, 3100, 2930, 1632, 1618, 1570, 1502, 792; ^1H ($CDCl_3$, 400 MHz) δ: 12.09 (*s*, 2′- and 2″-OH), 7.75 (*d*, $J = 8.1$ Hz, H-6′ and H-6″), 6.79 (*m*, H-3′ and H-3″), 6.73 (*ddd*, $J = 0.6$, 1.5, 8.1 Hz, H-5′ and H-5″), 3.45 (*s*, H-2 and H-3), 2.36 (*s*, 4′- and 4″ –CH_3); ^{13}C NMR ($CDCl_3$, 100 MHz) δ: 203.5 (C-1 and C-4), 162.5 (C-2′ and C-2″), 148.2 (C-4′ and C-4″), 129.7 (C-6′ and C-6″), 120.4 (C-3′ and C-3″), 118.5 (C-5′ and C-5″), 117.1 (C-1′ and C-1″), 31.6 (C-2 and C-3), 21.9 (C-4′- and C-4″ –CH_3); EI-MS *m*/*z* (rel. int.): 298 $[M]^+$ (36), 280 (4), 163 (83), 135 (100), 107 (7), 77 (10); HR-EI-MS *m*/*z*: 298.1201 $[M]^+$ (calc. for $C_{18}H_{18}O_4$, 298.1205).

4.4.2. Hofmeisterin III (4)

Oil; UV (CH_2Cl_2) λ_{max} nm (log ε): 228 (4.17); IR (film) ν_{max} cm^{-1}: 2962, 2870, 1734, 1224, 1128, 1036, 815; for ^1H ($CDCl_3$, 300 MHz) and ^{13}C ($CDCl_3$, 75 MHz) NMR spectra, see Table 2; EI-MS *m*/*z* (rel. int.): 232 $[M]^+$ (9), 149 (10), 135 (12), 105 (5), 83 (100), 55 (30); HR-EI-MS *m*/*z*: 232.1459 $[M]^+$ (calc. for $C_{15}H_{20}O_2$, 232.1463).

4.4.3. Hofmeisterin IV (5)

Oil; UV (CH_2Cl_2) λ_{max} nm (log ε): 269 (3.32); IR (film) ν_{max} cm^{-1}: 3349, 2924, 1719, 1230, 1154, 1045, 848; for ^1H ($CDCl_3$, 500 MHz) and ^{13}C ($CDCl_3$, 125 MHz) NMR spectra, see Table 3; FAB-MS *m*/*z* (rel. int.): 363 $[M + H]^+$ (3), 345 (17), 249 (15), 83 (100), 55 (73). HR-FAB-MS *m*/*z*: 363.1731 $[M + H]^+$ (calc. for $C_{20}H_{26}O_6$, 363.1729).

4.5. X-ray Analysis of hofmeisterin II (3)

Crystals (0.41 × 0.06 × 0.03 mm) were obtained from hexane. The crystal was monoclinic, space group $P2_1/c$, with cell dimensions $a = 9.895(3)$, $b = 4.768(1)$, $c = 16.513(4)$ Å, $V = 760.2(4)$ $Å^3$, $\rho_{calc.} = 1.303$ g/cm^3 for $Z = 2$, $M_W = 298.32$, and $F(0\,0\,0)e = 316$. The intensity data were measured on a Bruker Smart Apex CCD diffractometer equipped with graphite-monochromated Mo Kα radiation ($\lambda = 0.71073$ Å). Reflections, measured at 298(2) K within a 2θ range of 2.11–25.39°, were corrected for background, Lorentz polarization, and absorption ($\mu = 0.092$ $m\mu^{-1}$), while crystal decay was negligible. The structure was solved by direct methods and refined anisotropically by full-matrix least-squares on F2 using the SHELXL97 program (Sheldrick, 1998). For structural refinement, all atoms except hydrogens were refined anisotropically. The final discrepancy index was $R_F = 4.76\%$ using a unit weight for 1389 reflections and refining 103 parameters. The final difference Fourier map was essentially featureless, the highest residual peaks having densities of 0.149 $e/Å^3$. Crystallographic data for **3** are deposited with the Cambridge Crystallographic Data Centre (CCDC 646582). Copies of the data can be obtained, free of charge, on application to the Director, CCDC, 12 Union Road, Cambridge CB2 1EZ, UK. Fax: +44 (0) 1223 336033 or e-mail: deposit@ccdc.cam.ac.uk.

4.6. Molecular modeling

Geometry optimizations for compounds **1**–**5** were carried out using the MMFF94 force-field calculations as implemented in the Spartan 04 program. The systematic conformational search for the structures **1**–**5** was achieved with the aid of Dreiding models considering torsion angle movements of ca. 60°. The E_{MMFF} values were used as the convergence criterion, and a further search with the Monte Carlo protocol (Chang et al., 1989) was carried

without considering an energy cut-off. A selection of those minimum energy structures found between 0 and 3 kcal/mol were optimized by DFT at the B3LYP/DGDZVP level of theory (Godbout et al., 1992) using Gaussian 03W. Calculation of IR frequencies was achieved with the same level of theory at 298 K and 1 atm. No solvent effects were included in the calculations.

4.7. Phytogrowth-inhibitory bioassay

The phytogrowth-inhibitory activity of the crude extracts, fractions, and pure compounds was evaluated on seeds of *A. hypochondriacus*, *E. crus-galli* and *M. sativa* using a Petri dish bioassay (Pérez-Vásquez et al., 2005). In addition, a bioautographic phytogrowth-inhibitory bioassay was employed to guide secondary fractionation. The seeds of were purchased from Mercado de Tulyehualco, Mexico City, Mexico. The results were analyzed by ANOVA ($p < 0.05$) and IC_{50} values were calculated by probit analysis based on percent of either radicle growth or germination inhibition. Samples were evaluated at 10, 100 and 1000 $\mu g\,mL^{-1}$. Tricolorin A (Pereda-Miranda et al., 1993) was used as the positive control. The bioassays were performed at 28 °C during 24, 48 and 72 h for *A. hypochondriacus*, *E. crus-galli* and *M. sativa*, respectively.

Acknowledgments

This work was supported by grants from CONACyT and DGAPA-UNAM. We thank Rosa del Villar, Marisela Gutierrez and Georgina Duarte-Lisci for recording IR, UV, NMR, and mass spectra. Special thanks are due to Isabel Rivero and Laura Acevedo for their valuable technical assistance. A. Pérez acknowledges the scholarship awarded by CONACyT and DGEP-UNAM to carry out graduate studies.

References

Angelini, L.G., Carpanese, G., Cioni, P.L., Morelli, I., Macchia, M., Flamini, G., 2003. Essential oils from Mediterranean Lamiaceae as weed germination inhibitors. J. Agric. Food Chem. 51, 6158–6164.

Bohlmann, F., Dhar, A.K., Ahmed, M., 1980. Thymol derivatives from *Doronicum hungaricum*. Phytochemistry 19, 1850–1851.

Cerda-García-Rojas, C.M., Guerra-Ramírez, D., Román-Marín, L.U., Hernández-Hernández, J.D., Joseph-Nathan, P., 2006. DFT molecular modeling and NMR conformational analysis of a new longipinenetriolone diester. J. Mol. Struct. 789, 37–42.

Chang, G., Guida, W.C., Still, W.C., 1989. An internal-coordinate Monte Carlo method for searching conformational space. J. Am. Chem. Soc. 111, 4379–4386.

Godbout, N., Salahub, D.R., Andzelm, J., Wimmer, E., 1992. Optimization of Gaussian-type basis sets for local spin density functional calculations. Part I. Boron through neon, optimization technique and validation. Can. J. Chem. 70, 560–571.

Hernández-Romero, Y., Acevedo, L., Sánchez, M.D., Shier, W.T., Abbas, H.K., Mata, R., 2005. Phytotoxic activity of bibenzyl derivatives from the orchid *Epidendrum rigidum*. J. Agric. Food Chem. 53, 6276–6280.

Jiménez-Estrada, M., Velázquez, K., Lira-Rocha, A., Ortega, A., Díaz, E., Aumelas, A., Jankowski, K., 1989. Structure of a pentacyclic triterpenyl angelate from *Loeselia mexicana* proton 2D NMR data and stereochemistry. Can. J. Chem. 67, 2071–2077.

Joseph-Nathan, P., Wesener, J.R., Günther, H., 1984. A two-dimensional NMR study of angelic and tiglic acid. Org. Mag. Res. 22, 190–191.

Meazza, G., Scheffler, B.E., Tellez, M.R., Rimando, A.M., Romagni, J.G., Duke, S.O., Nanayakkara, D., Khan, I.A., Abourashed, E.A., Dayan, F.E., 2002. The inhibitory activity of natural products on plant *p*-hydroxyphenylpyruvate dioxygenase. Phytochemistry 59, 281–288.

Nguyen, T.D.T., Wanner, M.J., Koomen, G., Nguyen, X.D., 1993. New acetophenone and thymol derivatives from *Eupatorium stoechadosmum*. Planta Med. 59, 480–481.

Passreiter, C.M., Weber, H., Blaser, D.R., Boese, R., 2002. Stereochemistry and oxidative degradation thymol derivative from *Arnica sachalinensis*. Tetrahedron 58, 279–282.

Pereda-Miranda, R., Mata, R., Anaya, A.L., Wickramaratne, D.B., Pezzuto, J.M., Kinghorn, A.D., 1993. Tricolorin A, major phytogrowth inhibitor from *Ipomoea tricolor*. J. Nat. Prod. 56, 571–582.

Pérez-Vásquez, A., Reyes, A., Linares, E., Bye, R., Mata, R., 2005. Phytotoxins from *Hofmeisteria schaffneri*: Isolation and synthesis of 2′-(2′′-hydroxy-4′′-methylphenyl)-2′-oxoethyl acetate. J. Nat. Prod. 68, 959–962.

Román, L.U., del Río, R.E., Hernández, J.D., Joseph-Nathan, P., Zabel, V., Watson, W.H., 1981. Structure, chemistry, and stereochemistry of rastevione, a sesquiterpenoid from the genus *Stevia*. Tetrahedron 37, 2769–2778.

Sheldrick, G.M., 1998. Programs for Crystal Structure Analysis. Institut für Anorganische Chemie der Universität, Göttingen, Germany.

Tori, M., Ohara, Y., Nakashima, K., Masakuzo, S., 2001. Thymol derivatives from *Eupatorium fortunei*. J. Nat. Prod. 64, 1048–1051.

Valencia-Islas, N., Abbas, H., Bye, R., Toscano, R.A., Mata, R., 2002a. Phytotoxic compounds from *Prionosciadium watsoni*. J. Nat. Prod. 65, 828–834.

Valencia-Islas, N.A., Paul, R.N., Shier, W.T., Mata, R., Abbas, H.K., 2002b. Phytotoxicity and ultrastructural effects of gymnopusin from the orchid *Maxillaria densa* on duckweed (*Lemna pausicostata*) frond and root tissues. Phytochemistry 61, 141–148.

Veronneau, H., Greer, F., Daigle, S., Vincent, G., 1997. Use of mixtures of allelochemicals to compare bioassays using red maple, pin cherry, and American elm. J. Chem. Ecol. 23, 1101–1117.

Vokou, D., Douvli, P., Blionis, G.J., Halley, J.M., 2003. Effects of monoterpenoids, acting alone or in pairs, on seed germination and subsequent seedling growth. J. Chem. Ecol. 29, 2281–2301.